Synthesis of a New Composite Nanomaterial Consisting of Bentonite-Polyethylene Glycolphthalate / Original article

Lect. Dr. Tariq Yassin Mahmoud
College of Dentistry, Al-Esraa University, Baghdad / Iraq
dr.tariq@esraa.edu.iq

تخليق مادة نانوية متراكبة جديدة تتكون من البنتونيت ـ بولي إيثيلين جلايكول فثالات

م. د. طارق ياسين محمود
كلية طب الاسنان، جامعة الاسراء، بغداد \ العراق

Abstract

In this study, a new composite material was characterized and prepared by polymerizing ethylene glycol located among bentonite layers with phthalic anhydride. The results showed that the polymer bonds with the clay structure through hydrogen bonding. The polymerization process led to the destruction of the three-dimensional crystal structure of the clay and the isolation of its layers in the form of two-dimensional nanoscale shells. The growth of the polymer around the isolated clay layers increased the total particle size at the microscopic scale.

Keywords: Composite materials, Bentonite, Polyethylene glycol phthalate

المستخلص

حضرت و شخصت في هذه الدراسة مادة متراكبة جديدة من خلال بلمرة الاثلين كلايكول الموجود بين طبقات معدن البنتونايت مع مادة الفثالك انهايدرايد. بينت النتائج ان البوليمر يترابط مع هيكل الطيف من خلال التآصر الهيدروجيني. ادت عمليت البلمرة الى تحطيم التركيب البلوري ثلاثي الابعاد للطين وعزل طبقاته على شكل قشور نانوية ثنائية البعد، كما ان نمو البوليمر حول طبقات الطين المنعزلة عمل على زيادة الحجم الحبيبي الكلي للجسيمات عل المستوى المجهري.

الكلمات المفتاحية: مواد متراكبة، بنتونيت، فثالات بولي إيثيلين جلايكول

Introduction

Composite materials are formed from the union of two or more components has different properties from the other, those come together to form a new material differs in its properties from the parent materials, and a stable structure due to homogeneity of mixing at microscopic scale [1]. The composite consists of two basic elements, the binding medium or matrix and dispersed materials or additive. The binding material is the largest one which surrounds the other components and works to held all elements together producing a compact system. Additives are materials added to polymeric materials to give them specific properties and improving some other properties. These materials are added in the form of small granules or spheres. Additives to enhance the properties of polymeric materials by improving electrical conductivity [2], reducing or increasing porosity [3], maintaining dimensional stability, increasing the polymer's resistance to shocks [4], improving friction properties [5], and obtaining some magnetic properties [6-8]. The development of manufacturing clay minerals which are used as fillers allows obtaining thermoplastic materials with high mechanical strength. The approved method that was developed includes dispersing the filler granules in the polymer molten material after covering them with a thick layer of resin in which a very strong binding with the mold is achieved. The efficiency of clays in filling polymer systems also depends on the degree of their dispersion in the matrix medium, because well dispersion of the filler gives a higher surface area able to interact with the polymer frame [9].

In this work we amid to modify the surface of Iraq clay (Bentonite) by developing ester polymers and studying its morphology by scanning electron microscopy (SEM), Atomic force microscopy (AFM), diagnosing it by X- RD and FTIR.

Materials and Methods

Equipment uses

In this study, the raw materials and prepared materials were characterized using an X-ray Diffraction device, model 6000 shimaduz, Japan. Atomic force microscopy (AFM) type spam AA300 USA2008. FT-IR-600, Bio Tech U.K., England. SEM in the service laboratory of the College of Education for Pure Sciences / Ibn Al-Haitham. The work also included the use of the following devices during the preparation stage of the new composite material: a sensitive balance type Sartorius Lab. BL 210 S, Germany with ±0.0001g accuracy, laboratory furnace Green Equipment LTD, Melting Point Apparatus Galincamp England. Single Stage vacuum pump, China. Hyundai home microwave, 150 um sieve, Saxohlet device, and finally UV/VIS spectrometer, Double beam, shimadzu.1800, Japan.

Materials

The following chemicals were used in this research: Ethylene Glycol and Phthalic acid from BDH

Clay

Bentonite was obtained from the General Geological Survey Company. The the oxides percentages were (SiO_2: 54.66, CaO: 4.77, Al_2O_3: 14.65, MgO: 6.00, Fe_2O_3: 4.88, SO_3: 1.20, Na_2O: 0.65, loss on ignition: 12.56)

Bentonite preparation

The bentonite clay was washed with distilled water several times, then filtered and washed again using the Saxohlet device for a week to ensure the

removal of all ions present in the clay. The clay was dried using a laboratory oven at a temperature of 80 °C for two days until it was completely dry. Then, the bentonite was ground using a mortar mill and then the ground clay was sieved using a sieve with a diameter of 150 μm.

Preparation of Bentonite-Ethylene Glycol Complex B-EG

A (15 gm) of bentonite was placed in a beaker and gradually add (7 gm) of ethylene glycol in a mortar. The sample was ground continuously while adding ethylene glycol. The grinding process continued after the ethylene glycol was added for half an hour. The sample was covered tightly and left for 10 days to complete the diffusion process.

Preparation of Bentonite-Polyethylene Glycol Phthalate Compound

A (5 gm) of the previous complex (B-EG) was mixed with (5.5 gm) of freshly prepared phthalic anhydride (obtained from the thermal decomposition of phthalic acid under vacuum) in a mortar and the materials were ground until a homogeneous mixture was formed. This mixture was placed in the microwave for activation the polymerization condensation reaction for half a minute. After that, the mixture was taken out and ground again and returned to the microwave. This process was repeated until the sample hardened, then the time period was doubled to insure complete polymerization process. The obtained material was a homogeneous mass stable with microwave heating, does not dissolve in water and does not leave any trace of dissolved materials in water. This is confirmed by comparing the absorbance of the sample washing solution above with the absorbance of distilled water by UV/VIS spectrophotometer.

Results and Discussion

FT-IR Diagnosis

Figure (1) shows the FTIR spectrum of bentonite, the band appears at 3622 cm^{-1} is due to the stretching vibration of the (OH) group associated with the aluminosilicate structure in the clay. What distinguishes this (OH) group its presence in an environment with few hydrogen bonds, which make it appeared as a sharp band with a high frequency [10]. There is also another band at 3392 cm^{-1} due to the stretching vibration of the hydrogen-bonded (OH) groups, characterized by the shift to lower frequency and by an increase in the broadening of the absorption band [11] which due to the weakening of the (OH). At 1795 cm^{-1}, the bending vibration of the interlayer water molecules present between the clay sheets is noted [12]. At 1633 cm^{-1}, the stretching vibration of the carbonyl group in the carbonate radical is observed due to the presence of calcite mineral (calcium carbonate) impurities in the bentonite sample [13]. At 1007 cm^{-1}, a strong and broad band is observed due to the symmetric and asymmetric stretching vibrations of the aluminosilicate unit (Si-O-(Al)Si) [14]. Figure (2) shows the FTIR spectrum of the bentonite-ethylene glycol complex, where the free (OH) band is almost completely absent due to the hydrogen bonding between bentonite and ethylene glycol, at the same time, it is noticed a shift in the stretching frequency of the hydrogen-bonded (OH) group towards the higher frequency (blue shift) due to the contribution of the free (OH) group in the bentonite material, by hydrogen bonding, but this time with ethylene glycol molecules, this led to shifting the previous frequency of the hydrogen bonded of (OH) group towards the higher frequency. The weak band at 2983 cm^{-1} belongs to the stretching vibration of the aliphatic (C-H) bonds of ethylene glycol. The

bending vibration of the water molecule was shifted towards the higher frequency to reach 1847 cm^{-1}, which indicates that the (H_2O) molecule within the clay structure worked as a centers of receive ethylene glycol protons, which led to a decrease in the electronic density on the water oxygen atom and the appearance of a semi-positive molecular charge on it, which made the frequency to shift towards the higher frequency [15]. Also, the absorption band of the carbonyl group of (CO_3^{-2}) radical is shifted towards the higher frequency for the same reason. Also, the structural frame unit (Si-O-(Al)Si) band has shifted towards the higher frequency 1043 cm^{-1} combined by decrease band broadening, which means that the structural units (Si-O-(Al)Si) becomes more isotropic through the action of ethylene glycol molecules to increase the distances between the clay layers and thus reduce the molecular interactions between those clay layers which was the dominant case characterized by bentonite crystalline anisotropisity. After the polymerization of ethylene glycol molecules present between the clay layers in the bentonite mineral, as noticed in Figure (3) the return of the free (OH) group, but with a higher frequency than that of bentonite, which indicates the disengagement of the hydrogen bonding between the (OH) group and the ethylene glycol molecules. Also, a slight decrease in the frequency of the hydrogen-bonded (wide) (OH) group is observed due to the increase in hydrophobicity through the growth of the polymer between the bentonite mineral layers. As for the bending frequency band of the (H_2O) molecule, it remained the same, which indicates that it remains a center for receiving the few remaining protons that cause hydrogen bonding. We note that the stretching vibration of the new ester carbonyl group formed at 1765 cm-1 indicates that these groups act as centers for bonding with the protons that belong to the (OH) groups in the clay structure and thus have this high value.

As for the stretching vibrations of the carbonyl groups, they are present at 1618 cm^{-1}, as they shifted to a frequency lower than that of free bentonite due to the lack of opportunity for hydrogen bonding as a result of the competition of the nucleophilic polymer centers for hydrogen bonding. It is noted that the frequency of the building block (Si-O-(AL)Si) remains stable at 1043 cm^{-1}, which indicates that it has not entered into new bonds other than those that occurred during the formation of the bentonite-ethylene glycol (B-EG) complex, but the width of that band increases as a result of the increased randomness resulting from the positioning of the polymer between the clay layers.

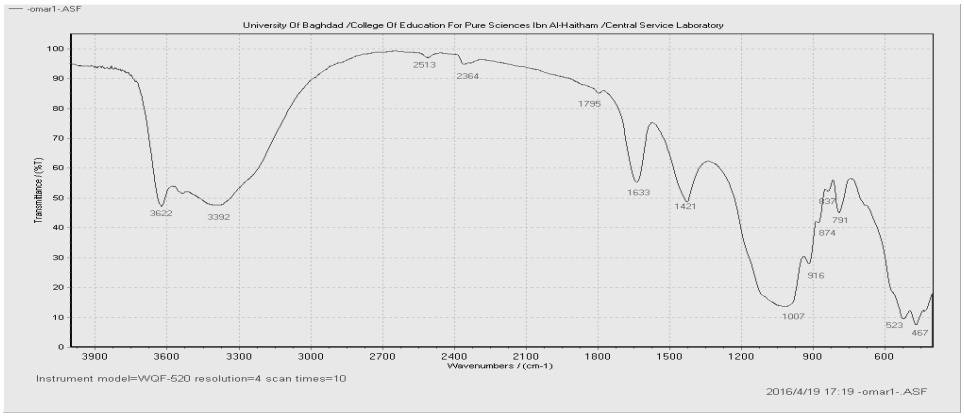

Figure (1) FTIR spectra of Bewntonite

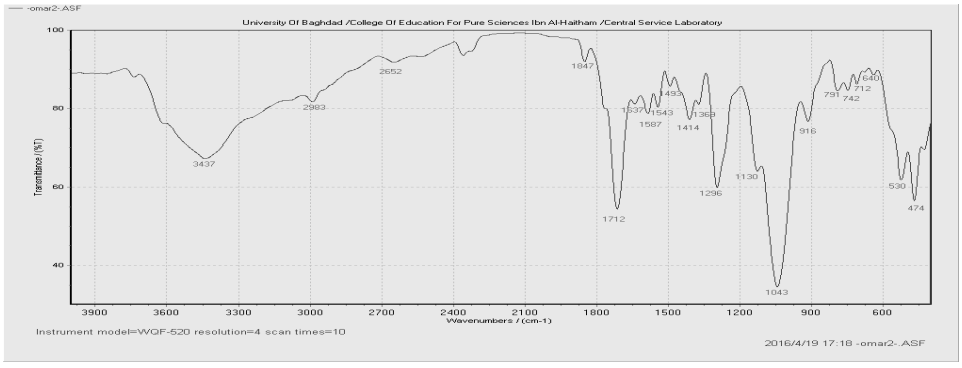

Figure (2) FTIR spectra of Bentonite-Ethyleneglycole complex

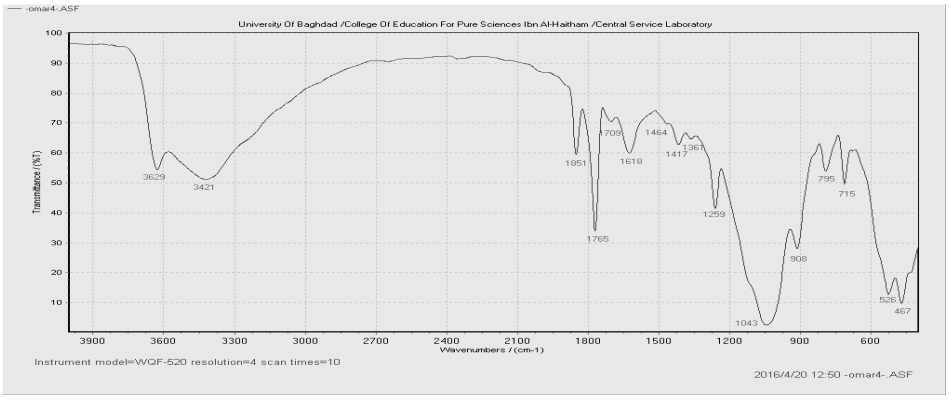

Figure (3) FTIR spectra of Bentonite-polyethylenglycol phthalate interlayer complex.

AFM Diagnosis

The results of the AFM for the bentonite model in Figures (4) and (5) show that the particle size of the particles ranges between (40-60nm) and the dominant diameter is at (90 nm) and the maximum height of the particles is (1.131 nm). The results for the modified bentonite mineral showed that the size distribution of the bentonite particles ranges from (60-130 nm) and the dominant diameter is at (75 nm) and the maximum height of the particles is (20.33 nm). After modification, it becomes clear that the polymerization process worked to increase the size of the bentonite particles through its positioning between its polymeric layers, in addition to its work to reduce the dispersion (poly dispersity) in the bentonite model. This means that the polymer worked to increase the homogeneity of the size distribution of the clay micro crystals. Increasing the homogeneity of the size distribution of the bentonite particles gives the surface desirable mechanical properties or electrical or thermal insulation properties similar to What is the case for the concept of (poly dispersity) for polymers.

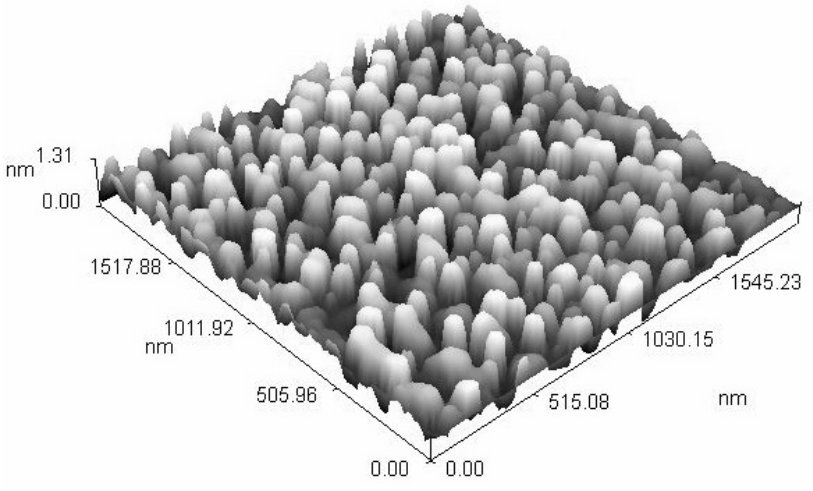

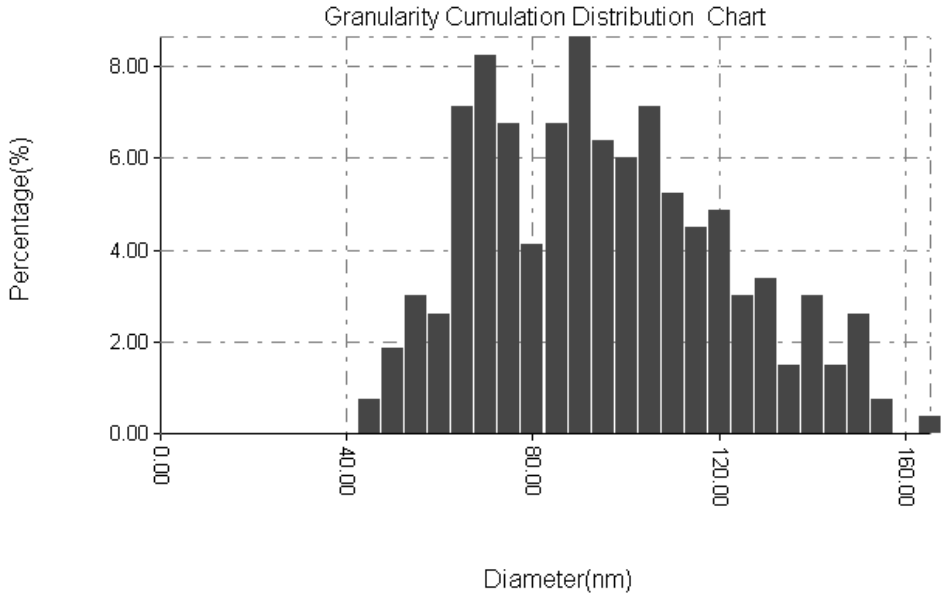

Figure (4) AFM picture and particle size distribution of the Bentonite

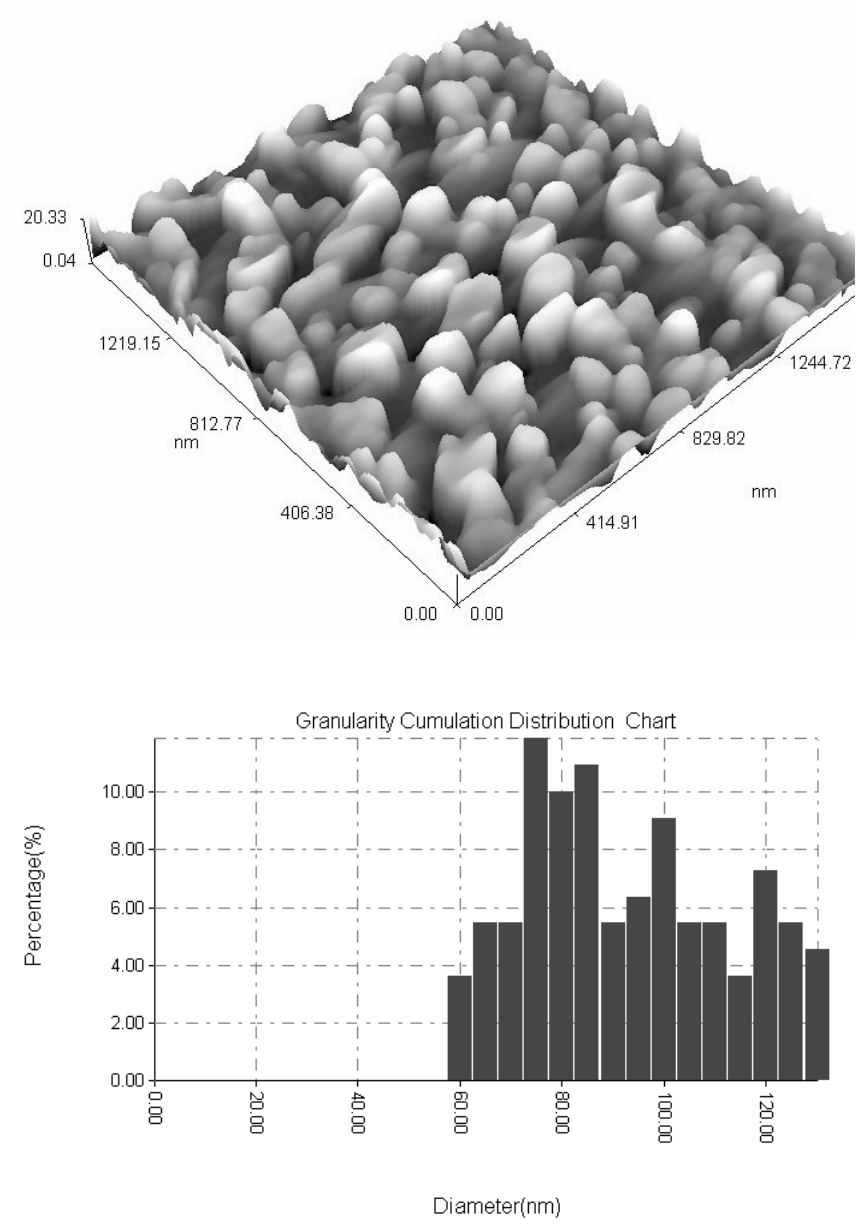

Figure (5) AFM picture and particle size distribution of the Bentonite-polymer composite

SEM Diagnosis

Figures (6) and (7) show the scanning electron microscope images of the bentonite sample before and after modification, which clearly shows what was previously indicated about increasing the homogeneity of the sample in the AFM diagnosis in terms of increasing the size of the small microscopic crystals through the growth of the polymer within the (100) plane, in addition to the destruction of very large crystals and their re-formation to reduce the variation in the sizes of these crystals, as the polymer appears as a fabric that increases the cohesion of the bentonite particles with each other.

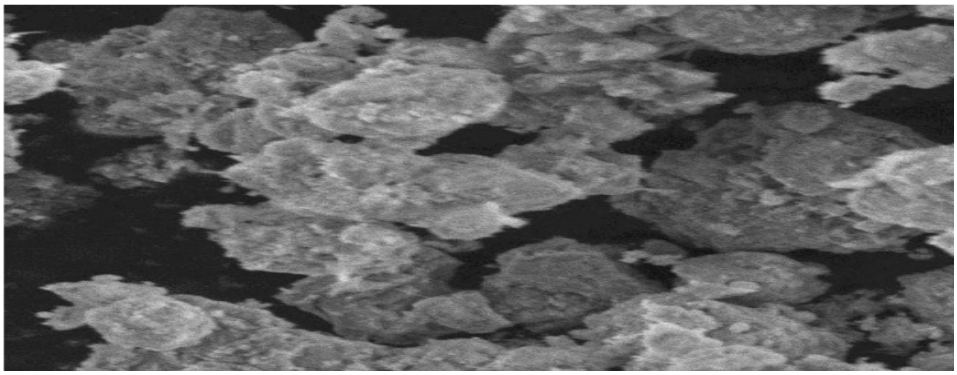

Figure (6) SEM image for the Bentonite

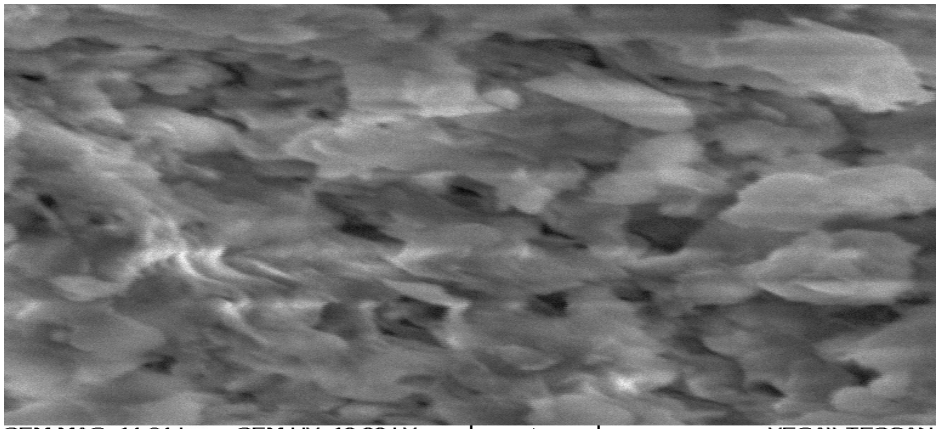

Figure (7) SEM image for the Bentonite-polymer composite

XRD Diagnosis

Montmorillonite constitutes the largest proportion in the composition of bentonite, as its crystal pattern is of the type (Mono clinic) and its crystal unit dimensions are (A = 5.717A^0, B = 8.94 A^0, C = 9.95 A^0) and the value of C varies according to the moisture and mineral content in the (001) plane [16]. Figure (8) shows that the (001) plane exists in the form of a wide band extending from the value of 2θ = 4.640 to 6.620, as the thickness of this plane ranges from 17.66 A^0 to 13.34 A^0. The reason for this dispersion is due to the lack of homogeneity of the bentonite sample in the content of cations and interlayer water content in the (001) plane [17]. The bentonite sample contained sand impurities (Q) with characteristic band at at 2θ=20.59, d=3.35 A^0 [18]. In the modified bentonite as shown in Figure (9) the band of the crystal plane (001) disappears due to the shift of this level to a higher (d) value below the detection limits of the device due to the growth of the polymer between the layers of this plane, which worked to increase the value of the expansion of this crystal level and thus its appearance at much lower values of 2θ. When reviewing the rest of the reflection multiples at this level, we note that they are not present, which means that the value of (d) expanded to infinity, meaning that the crystal peeled off at this level in a way that isolated the layers of the montmorillonite mineral in the form of two-dimensional sheet flakes [19]. It is also noted that the location of the crystal plane (100) was not affected as a result of polymerization, meaning that the polymerization process did not destroy the structure (octahedral and tatrahedra) in the single layers of aluminosilica, but rather worked to peel these layers and make them two-dimensional crystals with a length and width that did not change, but the arrangement of these layers along the height axis was destroyed. We also note

that silica or quartz were not affected by the polymerization process [20]. The basic units of montmorillonite are shown in Table No. 1.

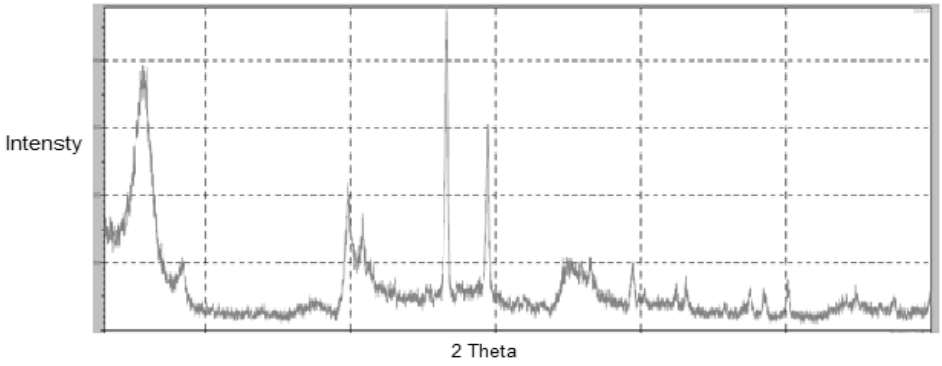

Figure (8) XRD pattern of the Bentonite

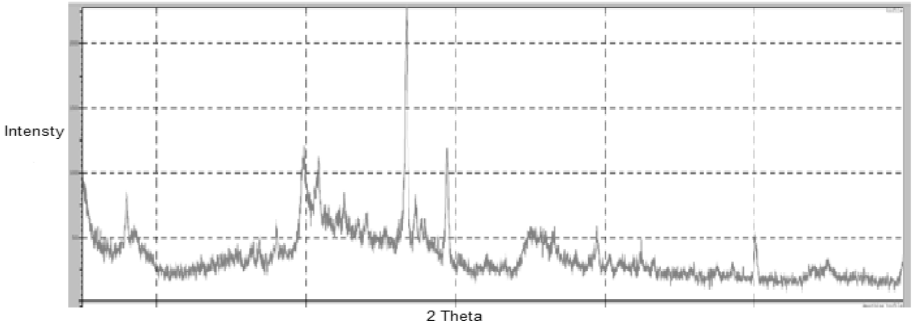

Figure (9) XRD pattern of the Bentonite-polymer composite

Table (1) Shows the basic units of montmorillonite mineral.

No		d-spacing	Hkl	I %
1	4.64-6.62	19-13.34	(001)	55
2	17.32	5.12	(003)	3
3	19.81	4.48	(100)	40
4	26.59	3.35	Q	100
5	29.40	3.04	$CaCO_3$	60
6	39.38	2.29	(007)	14

Conclusion

The obtained results indicate that the polymer (ethylene – glycol-phthalic anhydride) grow between the layer of the crystal plane (001) of the modified bentonite minerals due to the closure of active sites as a result of polymerization process.

References

1. Gürses, A., (2016), "Introduction to Polymer–Clay Nanocomposites", Taylor & Francis Group, LLC, 112-113 Turkey.
2. Fal, J; Bulanda, K; Oleksy, M; Żyła, G, (2024), "Effect of Bentonite on the Electrical Properties of a Polylactide-Based Nanocomposite.", Polymers (Basel), 16(10), 1372-1382.
3. Li, TT; Zhang, X; Wang, Z; Ren, HT; Peng, HK; Shiu, BC; *et al.*, (2021), "Study on Melamine/ Bentonite Polyurethane Porous Composite Foam: Pb^{+2} Adsorption and Mechanical Properties.", Ploy. Adv. Technol. [Internet]., 32(5), 2061–71.
4. Chen, J; Gustitus, S; Lin, H; Benson, C., (2022), "Shear Strength of Bentonite-polymer Composite Geosynthetic Clay Liners and Geomembranes.", Environmental Geotechnics., 11,1–10.
5. Kapitonova, I; Lazareva, N; Tarasova, P; Okhlopkova, A; Laukkanen, S; Mukhin, V,(2022), "Morphology Analysis of Friction Surfaces of Composites Based on PTFE and Layered Silicates.", Polymers (Basel) [Internet]., 14(21), 1-16.
6. **Hernández-Hernández, K.; Illescas, J.; Díaz-Nava, M.; Muro-Urista, C.; Martínez-Gallegos, S. and Ortega-Aguilar, R.**, (2016), " Polymer-Clay Nanocomposites and Composites: Structures, Characteristics, and Their Applications in the Removal of Organic Compounds of Environmental Interest", Medicinal Chemistry, 6(3), 201-210.
7. Sankar, K. and Krishnan, A., (2016), "Property Evaluation of Polypropylene Hybrid Composite with Nano Clay", International Journal of Innovations in Engineering and Technology (IJIET), 6(4), 479-483.
8. Mansri, A.; Bendraoua, A. and Bouras, B., (2016), "Polyacrylamide-clay Microcomposite as Corrosion Inhibitor for Mild Steel in 1m Hydrochloric Acid Solution", 7(3), 808-819.
9. Kumar, R. and Rao, S., (2011), "Effect of Substrate Temperature on Structural Properties of Nanostructured Zinc Oxide Thin Film by Reactive DC Magnetron Sputtering", Digest Journal of Nanomaterials and Bio structures, 6(3), 1281-1287.

10. Abramczyk, H., (1993), “Infrared Absorption in Hydrogen-bonded Complexes and Absorption of an Excess Electron in Hydrogen-bonded Solvents”, Vibrational Spectroscopy, 5, 109-117.

11. McMillan, P. and Remmele, R., (1968), “Hydroxyl Sites in SiO_2 Glass: A Note on Infrared and Raman Spectra”, Americam Mineralogist, 71, 772-778.

12. Che, C.; Glotch, T.; Bish, D.; Michalski, J. and Xu, W., (2011), “Spectroscopic Study of the Dehydration and/or Dehydroxylation of Phyllosilicate and Zeolite Minerals”, Journal of Geophysical Research, 116, 376.

13. Weir, C. and Lippincott, E., (1961), “Infrared Studies of Aragonite, Calcite, and Vaterite Type Structures in the Borates, Carbonates, and Nitrates”, Journal of Research of the National Bureau of Standards-A. Physics and Chemistry, 65A(3), 57-68.

14. Zarubin, D., (1999), “Infrared Spectra of Hydrogen Bonded Hydroxyl Groups in Silicate Glasses. A Re-Interpretation”, Phys. Chem. Glasses, 40(4), 184-192.

15. Joseph, J. and Jemmis, E., (2007), "Red-, Blue-, or No-Shift in Hydrogen Bonds: A Unified Explanation", Jour. Amer. Chem. Soc.", 129, 4620-4632.

16. Ross, C. and Hendricks, S., (1943), “Minerals of The Montmorillonite Group", Geological Survey Professional Paper A, 205, 23-79.

17. Breen, C., (1985), “Review of the Diffusion of Water and Pyridine in the Interlayer Space of Montmorillonite”, Clay and Clay Minerals, 33(4), 275-284.

18. Morris, M.; McMurdie, H.; Evans, E.; Paretzkin, B.; Parker, H. and Panagiotopoulos, N., (1981), “Standard X-ray Diffraction Powder Patterns”, National Bureau of Standards, USA.

19. Tao, L.; Xiao-Feng, T.; Yu, Z. and Tao, G., (2010), “Swelling of K^+, Na^+ and Ca^{+2}-Montmorillonites and Hydration of Interlayer Cations: A Molecular Dynamics Simulation”, Chin. Phys. B, 19(10), 109101-07.

20. Fusova, L., (2009), "Modification of the Structure of Ca-Montmorillonite", GeoScience Engineering, 15(1), 27-32.